Proceedings of ASME Turbo Expo 2025
Turbomachinery Technical Conference and Exposition
GT2025
June 16–20, 2025, Memphis, Tennessee, USA

GT2025-153615

EFFICIENCY ENHANCEMENT IN PRESSURE GAIN COMBUSTION COMBINED CYCLE GAS TURBINE BY BLADE COOLING INTEGRATION WITH BOTTOMING CYCLE

Abhishek Dubey
Thermochemical Power Group (TPG)
University of Genova,
16145 Genova, Italy
abhishek.dubey@edu.unige.it

Alessandro Sorce
Thermochemical Power Group (TPG)
University of Genova,
16145 Genova, Italy
alessandro.sorce@unige.it

Aristide Fausto Massardo
Thermochemical Power Group (TPG)
University of Genova,
16145 Genova, Italy
aristide.massardo@unige.it

ABSTRACT

This paper investigates the potential advantages of integrating turbine blade cooling with bottoming cycle in Combined Cycle Gas Turbine (CCGT) with Pressure Gain Combustion (PGC) for land-based power generation application. PGCs have recently emerged as a promising solution to achieve significant performance gains in current Gas Turbines (GT) and CCGTs in terms of efficiency and power output. However, GTs with PGC combustors require higher cooling flow compared to conventional GTs, due to the increased temperature of cooling flow from its secondary compression that is necessary for admission in the turbine. The present work aims to address this issue by utilizing the working fluid from the steam cycle for cooling stator and rotor vanes or to decrease the cooling air temperature. PGC is represented by a steady-state zero-dimensional constant volume combustion (CVC) model based on the Humphrey cycle. The PGC combustor model is simulated with different injection pressure losses to investigate the impact of pressure gain on steam cooling integrated CCGT. Different approaches of turbine blade cooling through the bottoming cycle are investigated in this work, such as (i) cooling of compressor bleed air through steam/water, ii) open-loop steam cooling (OLSC) for stator and vanes, iii) closed-loop steam cooling (CLSC) for stator and vanes and iv) mixed loop steam cooling (MLSC) where stator is steam cooled while rotor is air cooled. A heavy-duty industrial H-class CCGT with a PGC combustor and a three-pressure level heat recovery steam generator (HRSG) was modelled in WTEMP (Web-based Thermo-Economic Modular Program) software, an original modular cycle analysis tool developed at the University of Genova. Thermodynamic analysis of the CCGT cycle was performed with realistic component efficiencies at a wide range of operating conditions, with methane as the fuel. The impact of different cooling approaches on the cycle performance was analyzed in terms of efficiency, specific work and practical feasibility of the solution. Results showed that implementing both PGC technology and steam cooling together in a CCGT can significantly enhance efficiency and work output due to the synergistic effect of both technologies. The efficiency of an H-class CCGT can be increased from 62.6 to 67.2% (4.54 percentage points increment) and specific work by 194.5 kJkg$_{air}$ by using CLSC and PGC combustor with a pressure gain of 0.40. MLSC was identified as the most practical solution, which, when augmented with a PGC combustor with 0.26 pressure gain, can improve the overall CCGT efficiency by 2.9 percentage points and specific work by 104.6 kJ/kg$_{air}$. Overall, the study demonstrates the theoretical potential of integrating turbine cooling in the PGC combined cycle with steam bottoming cycle as a potential pathway towards CCGTs with more than 65% efficiency.

Keywords: gas turbine, pressure gain combustion, Humphrey cycle, constant volume combustion, combined cycle, efficiency, steam cooling, turbine blade cooling

NOMENCLATURE

Symbols

Bi_{met}	biot number of turbine blade metal
Bi_{TBC}	biot number of thermal barrier coating
c_p	specific heat capacity [Jkg^{-1}K^{-1}]
ε_o	cooling effectiveness
ε_f	film cooling effectiveness
K_{cool}	cooling flow factor
η_{int}	internal convective cooling efficiency
m	mass flow rate [kgs^{-1}]
P_{gain}	combustor pressure gain
Q	heat [J]
T	temperature [K]
ε_f	film cooling effectiveness
Ψ	cooling flow ratio

Subscripts

a	air
adwall	adiabatic wall
ca	cooling air
cs	cooling steam
comb	combustor
bl	turbine blade
g	main gas flow in turbine

in	inlet
out	outlet
p.p.	percentage points
Acronyms	
3PRH	three pressure level with reheat
BC	bottoming cycle
CPR	compressor pressure ratio
CLSC	closed loop steam cooling
CBAC	compressor bleed air cooling
CVC	constant volume combustion
DEA	deaerator
EC	economizer
EV	evaporator
HRSG	heat recovery steam generator
HP	high-pressure level
IP	intermediate-pressure level
GT	gas turbine
LP	low-pressure level
LHV	lower heating value of fuel [Jkg^{-1}]
MLSC	mixed loop steam cooling
OEM	original equipment manufacturer
OLAC	open loop air cooling
OLSC	open loop steam cooling
PGC	pressure gain combustion
ST	steam turbine
SH	superheater
TIT	turbine inlet temperature [K]
TOT	turbine outlet temperature [K]

1. INTRODUCTION

Pressure gain combustion (PGC) is a promising technology to achieve major performance improvements in current open-cycle gas turbines (GT) and combined-cycle gas turbines (CCGT) [1–7]. A PGC gas turbine has a pressure rise in the cycle heat addition process that increases efficiency and power output. However, this technology is practically challenging mainly due to the fundamentally unsteady and periodic nature of the PGC combustion that produces pulsating outflow and makes its integration with steady turbomachinery difficult [4]. Furthermore, the unsteady PGC combustion also presents challenges in developing its reduced order models for steady cycle analysis [8]. Other practical challenges with PGC include ignition, mixing, valving, deflagration to detonation transition and thermal management. Nevertheless, due to its immense theoretical potential, a significant amount of research efforts are being devoted towards addressing the challenges in PGC technology at both, component and cycle level [7,9,10].

The advantages of GTs with PGC combustors have been shown in several past studies. In one of the earliest studies, Heiser et al. [11] performed an air-standard real cycle analysis of open cycle GT and quantified the efficiency benefits from PGC due to pressure rise in combustion. Subsequently, Stathopoulos [12] conducted a more realistic analysis of open cycle GT based on PGC with practical losses from turbine cooling, secondary air compressor, constant pressure combustion loss and reduced turbine performance using a constant volume combustion (CVC) based PGC model developed by Nalim [13]. It was found that the Humphrey cycle will most probably make sense for turbine inlet temperatures above 1500°C and pressure ratio less than 25, but with very high losses in PGC combustor, the attainable performance benefits from PGC can be completely lost [12]. Moreover, a PGC cycle with high TIT was found to alleviate the effect of practical losses better than a low TIT cycle. Similar effects in PGC open cycle GT were also reported recently by Dubey et al. [7].

At present, CCGTs are the most efficient technology to produce electricity from fossil fuels with efficiencies approaching 64% [14,15]. However, the technology has reached an asymptotic limit for further improvements with conventional combustor and blade cooling approaches. PGC technology is one such solution to increase CCGT performance, and the potential benefits have been shown in past research. For instance, Gulen [16] conducted a real cycle analysis of PGC based on pulsed detonation combustion (PDC) in 505.3 MW CCGT with an air-cooled J-class industrial GT at a pressure ratio of 23 and TIT of around 1600 °C at pressure gain conditions. At a combustor pressure ratio of 1.85, an efficiency increment of 3.3 p.p. (percentage points) and a CCGT power increment of 74.4 MW over the baseline CCGT were achieved [16]. Similarly, Holley also studied an air-cooled CCGT with PDC and RDC models by accounting for unsteadiness in heat addition. Results showed an efficiency increase of around 1.9 p.p. and 2.6 p.p. and an increase in CCGT power of 3.1% and 4.1%, with PDC and RDC, respectively [17]. Giuffrida et al. [18] investigated an F-class CCGT with PGC at design point conditions with three different values of combustor pressure rise and different cooling flows. With a 45% pressure rise in the combustor and 10% cooling bleed, the GT power and efficiency increased by 47 MW and 2.9 p.p., respectively. The corresponding increase in CCGT power and efficiency was 48.9 MW and 2 p.p., respectively. More recently, a comprehensive analysis of CCGT with PGC combustor with realistic, practical losses was performed by the authors at a wide range of operating conditions [7]. It was shown that the gain in the topping cycle from the PGC combustor is higher than the loss in the bottoming cycle from reduced TOT, and so the total power and efficiency of PGC-CCGT are always higher than the conventional one. Also, as TOT in PGC-CCGT increased with practical losses, loss in CCGT power was partially reduced due to bottoming cycle recovery. For a 1700°C TIT and compressor pressure ratio of 25, using PGC could increase CCGT efficiency by more than 3 p.p., in the optimistic case, without practical losses. It was also found that the optimum compressor pressure ratio for maximum efficiency in PGC-CCGT was less than that of the conventional one at all design conditions [7].

An important aspect of the PGC GT cycle is that it requires additional compression of cooling air from the compressor to overcome the pressure gain in the combustor for entry into the turbine. This secondary compression increases the cooling flow temperature, which increases the amount of cooling flow required for the same heat transfer from the blade [12,18,19]. Thus, in conventional configuration with open loop air cooling, PGC cycles have higher cooling flow than conventional GT and more importantly, the cooling flow increases with pressure gain. For example, in the results reported by Stathopoulos [12], the total compressor cooling bleed percentage for Joule and PGC cycles was 15.4% and 20.4%, respectively, at pressure ratio of 25 and TIT of 1700°C. Similarly, at the same operating conditions, the cooling bleed percentage for the Joule cycle was 17.6%, but that for PGC was 19.9% and 18.8% for optimistic and realistic cases, respectively, in a recent work by authors [20].

Apart from PGC technology, CCGT performance can also be improved by using steam from the bottoming cycle for turbine cooling, which reduces the cycle efficiency penalty associated with blade cooling. Due to its superior heat exchange properties, lower entry temperature than air and higher specific heat, using steam as a cooling medium requires less cooling flow compared to compressor bleed air [21,22]. Additionally, steam from the bottoming cycle can be used to cool the compressor bleed air before entry into the turbine, and it can be used to cool the turbine blades in open and closed configurations directly. In all methods, the additional heat from the topping cycle is transferred in the bottoming cycle through turbine blades, which increases bottoming cycle work and reduces cooling associated penalty on topping cycle performance.

In one of the earliest studies pertaining to steam integration with bottoming cycle, Watson [22] reported an efficiency rise of 1.1 p.p. by replacing conventional open loop air cooling (OLAC) in the first nozzle with closed loop steam cooling (CLSC). Also, upto 2 p.p. efficiency rise was estimated by replacing the cooling of all rows with closed loop steam cooling [22]. Ghigliazza et al. [23] reported an increase in efficiency and total power of 2 p.p. and 121.7 MW by replacing conventional open-loop air cooling with closed-loop steam cooling for turbine blades in a 459 MW CCGT. Chiesa et al. [24] performed a detailed comparison of conventional open-loop air cooled with closed-loop steam and mixed air/steam cooling in CCGT with 1430°C TIT. Results showed an efficiency increase of 1.8 p.p. by closed-loop steam cooling and an additional increase of 0.9 p.p. by adding sequential combustion with steam cooling [24]. Similarly, mixed loop steam cooling, in which the stator was cooled by steam and the rotor by air, increased efficiency by 1.54 p.p. Moreover, both closed and mixed loop cooling led to a significant increment in CCGT power by around 13.5%. Kotowicz et al. [25] also demonstrated CCGT efficiency improvements of around 3 p.p. by cooling the compressor bleed air to 100°C with bottoming cycle fluid in an additional heat exchanger. Sanjay et al. [26] performed a parametric analysis of different cooling solutions in CCGT and found that, unlike conventional air-cooled cycles, cycle efficiency in the case of closed-loop steam cooling continues to increase with TIT without exhibiting maxima. This behaviour is also consistent with results presented by Chiesa et al. [24], and it indicates the importance of closed-loop steam cooling in high TIT cycles. Recently, Kotowicz et al. [27] observed that the CCGT efficiency with closed-loop steam cooling increases with compressor pressure ratio at all ranges, unlike air-cooled configuration, where it shows maxima with TIT. It must be noted that all these steam cooling integration studies have been performed in CCGT with conventional isobaric combustors.

Turbine cooling integration with bottoming cycle steam has some practical challenges as well. Firstly, cooling integration with the steam cycle reduces plant flexibility and makes startup difficult, necessitating additional steam generators for turbine cooling during startup, which decreases the ramp rate of the CCGT [27]. Secondly, closed-loop steam cooling can subject the blades to high thermal gradients if the steam entry temperature is very low [22]. Finally, the trailing edges of the blades always require some form of open loop cooling due to low thickness. In some cases, there can also be environmental limitations depending on water availability. Despite these difficulties, OEMs have made attempts to implement steam cooling in practical systems. Mitsubishi Heavy Industries has implemented steam cooling for turbine blades and combustor in its M501G units [28]. General Electric has also introduced steam-cooled gas turbines in its STAG-107H and STAG-109H CCGT units [29].

This work aims to understand the performance improvement in modern CCGTs with both, PGC combustor and turbine blade cooling integrated with the bottoming cycle. To date, PGC technology and steam cooling integration have been studied as two independent solutions for performance improvement in CCGTs, and a study related to the combined impact of both technologies is not available in the open literature. To the best of the author's knowledge, the current study is the first attempt to study performance enhancement from turbine cooling integration with bottoming cycle in CCGTs with PGC combustion. Theoretically, steam cooling offers a solution to address the issue of high cooling flow in the topping cycle with a PGC combustor.

This paper is structured as follows: first, the pressure gain combustion model is described, followed by the validation of the CCGT model and different layouts for steam cooling integration. After that, results are discussed, and performance improvements from each steam integration strategy are analyzed at different values of pressure gain.

2. METHODOLOGY

2.1. Pressure Gain Combustion Model

Pressure gain combustion in this work is represented by a constant volume combustion (CVC) model developed by Nalim [13] that has been used in recent PGC studies [7,12,20]. Figure 1 shows the PGC model on the temperature-specific entropy diagram. As per the model, the PGC combustion consists of a pure CVC process (2-3a) followed by an internal expansion (3a-3b), which does not produce cycle work and generates a steady state at the combustor outlet from the unsteady and periodic CVC process. This internal expansion is important as it avoids overestimation of cycle work and thus, performance, which would otherwise result if the work is extracted from the momentarily occurring maximum temperature in the unsteady CVC process [7]. The process 3b-4 in Fig. 1 is the turbine expansion for cycle work generation.

This PGC model aims to represent the time-dependent process by a thermodynamically equivalent steady process in an open cycle. To achieve this, the flow work required to expel the products of the pure CVC process (3a) to the equivalent steady state at the combustor outlet (3b) is accounted for through the internal expansion (3a-3b). Based on the model, it is also assumed that the overall combustion process 2-3b represents heat addition in a steady and open thermodynamic system [10,12]. This way, the model generates pressure gain while maintaining the enthalpy balance across the combustor.

With inlet conditions known at state 2, T_{3b}, which is the outlet temperature of the PGC combustion process, is calculated by applying enthalpy conservation across the combustor. T_{3a}, the temperature at the end of the pure CVC process, is calculated through the conservation of internal energy. Pressure at the end of pure constant volume combustion, P_{3a} is then calculated with the perfect gas equation using the assumption of constant specific

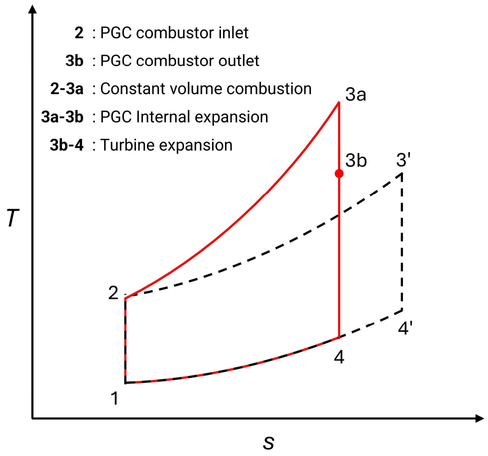

FIGURE 1: TEMPERATURE - SPECIFIC ENTROPY DIAGRAM OF THE PGC MODEL BASED ON HUMPHREY CYCLE

volume for pure CVC process. With T_{3a}, P_{3a} and T_{3b} known, P_{3b}, which is the outlet pressure of the PGC combustion process, is calculated by modelling process 3a-3b as an adiabatic expansion, where the value of γ is iteratively estimated at the average temperature of the expansion process. A more detailed description of this PGC model calculations can be found in the recent work of the authors [7,20]. The non-dimensionalized pressure gain, P_{gain}, can then be calculated by Eq. (1).

$$P_{gain} = \frac{P_{comb,out}}{P_{comb,in}} - 1 \tag{1}$$

In this work, the working fluid is a mixture of five gases: N_2, O_2, H_2O, CO_2 and Argon. For each gas mixture, enthalpy was defined as the sum of the enthalpy of formation and sensible enthalpy. The total mixture enthalpy was calculated based on the individual gas mass fractions while accounting for specific heat variation with temperature. The mixture composition of combustion products was determined using species conservation for the given equivalence ratio.

2.2. Turbine Cooling Model

For each turbine stage, the cooling flow ratio was separately calculated for the stator and the rotor. The expansion process of a cooled turbine stage is shown in Fig. 2. In the first step, the stator cooling air is mixed with the main gas flow, and the resulting mixture is expanded in the rotor. A mixing pressure drop equal to 0.07Ψ was considered for the mixing of the main gas flow and cooling flow in the stator based on the correlation developed by Horlock et al. [30]. The cooling air for the rotor is mixed after the expansion, and the resulting mixture enters the subsequent stage. This model of turbine expansion with stator and rotor cooling is widely implemented in literature and is effectively able to capture practical trends [12,31].

The cooling flow was estimated based on the approach developed by Wilcock et al. [32]. It allows the prediction of cooling flow ratio (Ψ) based on different cooling technology levels (CTL) expressed in terms of five parameters (Eqs. 2-6) namely cooling flow factor (K_{cool}), internal convective cooling efficiency (η_{int}), film cooling effectiveness (ε_f), Biot number of turbine blade metal (Bi_{met}) and Biot number of thermal barrier coating (Bi_{TBC}). For a given main gas temperature (T_g), allowable blade metal temperature (T_{bl}) and cooling flow inlet temperature

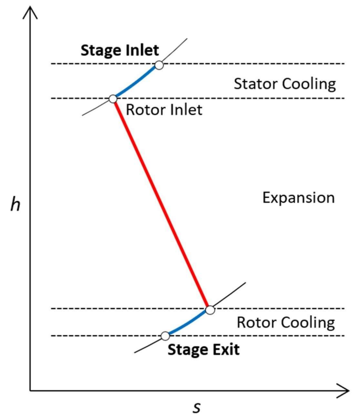

FIGURE 2: EXPANSION MODEL OF A COOLED TURBINE STAGE [7]

($T_{ca,in}$), the cooling effectiveness (ε_o) is calculated by Eq. 2, and then, Ψ is estimated from Eq. 6 using the parameters listed in Table 1 for the given cooling technology.

$$\varepsilon_o = \frac{(T_g - T_{bl})}{(T_g - T_{ca,in})} \tag{2}$$

$$\eta_{int} = \left(\frac{T_{ca,out} - T_{ca,in}}{T_{bl} - T_{ca,in}}\right) \tag{3}$$

$$\varepsilon_f = \left(\frac{T_g - T_{adwall}}{T_g - T_{ca,out}}\right) \tag{4}$$

$$Bi = Bi_{TBC} - Bi_{met}\left(\frac{\varepsilon_o - \varepsilon_f}{1 - \varepsilon_o}\right) \tag{5}$$

$$\Psi = \frac{m_{ca}}{m_g} = \frac{K_{cool}}{(1+Bi)}\left(\frac{\varepsilon_o - \varepsilon_f\,[1 - \eta_{int}(1-\varepsilon_o)]}{\eta_{int}(1-\varepsilon_o)}\right) \tag{6}$$

In real turbines, K_{cool} is a function of complex flow and blade geometry parameters such as surface area, mean heat transfer coefficient and Stanton number. For convenience, Wilcock et al. [32] considered a constant value of K_{cool}, which was calibrated with real engine data.

TABLE 1: PARAMETERS OF BLADE COOLING MODEL USED IN THIS WORK

Parameter	Symbol	Value
Cooling flow factor	K_{cool}	0.045
Internal convective cooling efficiency	η_{int}	0.70
Film cooling effectiveness	ε_f	0.40
Biot number of blade metal	Bi_{met}	0.15
Biot number of thermal barrier coating	Bi_{TBC}	0.30

Moreover, to account for the non-uniformity of temperature at the combustor outlet, the main gas temperature at the first stator inlet was modified as per Eq. 7 for calculating Ψ [32].

$$T_{g,max} = T_g + K_{comb}\,\Delta T_{comb} \tag{7}$$

where $T_{g,max}$ is the maximum temperature at the inlet of the first stator, K_{comb} is the pattern factor and ΔT_{comb} is the combustor temperature rise. The value K_{comb} was 0.15, the same as the one used by Wilcock [32].

It is important to mention that this model for predicting cooling flow was developed for conventional open loop air cooling through compressor bleed air. Therefore, the effect of heat exchange properties of air as the cooling medium was accounted for within the model. In order to use this model for steam, which has higher specific heat, the cooling flow ratio with steam was calculated, keeping the heat transferred from the blade to the cooling medium the same as that with air. Once the cooling flow ratio was calculated with air, $T_{ca,out}$ which is the temperature of cooling air exiting the blade, was obtained from Eq. 3. Next, Q_{bl}, heat transferred from blade to cooling air, was calculated from heat balance in turbine blade system as per Eq. 8.

$$Q_{bl} = m_{ca}(c_{p,ca,out}T_{ca,out} - c_{p,ca,in}T_{ca,in}) \quad (8)$$

where m_{ca} is the mass flow of cooling air, $c_{p,ca,out}$ and $c_{p,ca,in}$ are the specific heats for cooling air at the outlet and inlet of the blade, respectively. Thereafter, m_{cs}, the mass flow of cooling steam required to transfer Q_{bl} amount of heat, was calculated from Eq. 9. The temperature of the cooling steam at the blade exit was the same, as defined by the value of η_{int} in Eq. 3.

$$Q_{bl} = m_{cs}(c_{p,cs,out}T_{cs,out} - c_{p,cs,in}T_{cs,in}) \quad (9)$$

This approach allowed capturing the effect of higher specific heat of steam in terms of reduced cooling flow. This reduced cooling flow of steam compared to air is shown in Fig. 3 for the stator and rotor of the first turbine stage (as a percentage of main gas flow) at different TIT values for the same cooling fluid inlet temperature and blade metal temperature.

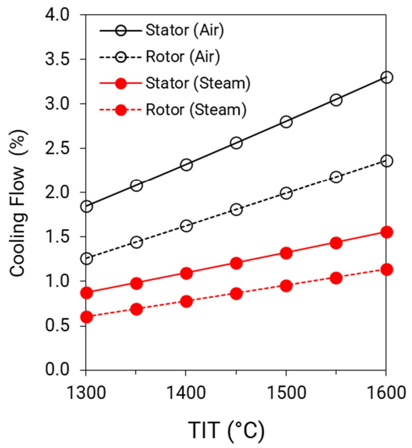

FIGURE 3: REPRESENTATIVE COOLING FLOW WITH AIR AND STEAM AS COOLING MEDIUM: $T_{ca,in} = T_{cs,in} = 212.4$°C AND $T_{bl} = 825$°C.

Just like in the case of OLAC (Fig. 2), the steam was mixed with the main gas flow before and after the expansion for the stator and rotor, respectively, in OLSC. In CLSC, a Q_{bl} amount of heat was transferred from the main gas to steam through the turbine blade, and thus, the main gas enthalpy was reduced by Q_{bl} as per Eq. 10. Thereafter, cooling steam exited the turbine row without mixing.

$$Q_{bl} = m_g(c_{p,g,in}T_{g,in} - c_{p,g,out}T_{g,out}) \quad (10)$$

2.3. CCGT Model Validation

To study the impact of the PGC combustor with steam cooling in a CCGT power plant, a CCGT with a gas turbine cycle consisting of four turbine stages connected to a 3PRH bottoming cycle was modelled in the WTEMP software. Each turbine stage consisted of one stator row and one rotor row. This CCGT layout was then validated with the nominal design point specifications of the latest H-Class 50 Hz industrial CCGT power plant from major original equipment manufacturers (OEMs). WTEMP was used for all the simulations performed in this work. It is a modular and flexible tool for thermo-economic analysis and optimization of innovative energy systems. It is used here because of its upgradability and extensive implementation in the past for advanced gas turbine cycles [7,33,34].

Performance specifications for Ansaldo GT36-S5 and Mitsubishi M701JAC were acquired from the Turbomachinery International handbook 2024 [35], while those for General Electric (GE) 9HA.02 were obtained from the OEM website [15]. In general, rating specifications disclosed by OEMs are limited to CPR, exhaust mass flow, TOT, efficiency (LHV basis) and power output for simple cycle and combined cycle plants [36]. All OEM ratings are provided at ISO baseload conditions (15°C, 1 atm and 60% relative humidity) and 100% methane fuel with fuel preheating and 3PRH HRSG configuration. However, several important parameters required for modelling these CCGTs, such as TIT, cooling flow, BC pressure levels, condenser pressure, heat losses and auxiliary losses, are not disclosed as they are propriety information of OEMs. Therefore, for theoretical validation of these plants, one is forced to make reasonable assumptions for unknown parameters [24,36]. For validating these models in WTEMP, all available input parameters from OEM, such as inlet conditions and compressor pressure ratio were maintained the same as reported by OEM. The values of other unavailable cycle parameters were calibrated to minimize the difference in performance parameters (electrical efficiency and power) between the WTEMP model and practical CCGT. The values of the calibrated parameters were kept within the reasonable practical range based on information available in the literature. All calibrated parameters were kept the same for three CCGTs, and values are listed in Table 2 and Table 3 for the GT cycle and steam cycle, respectively. This is the typical approach for validating complex CCGT models with real power plants [18,24,36], and a more detailed description of such an approach and associated challenges can be found in the work done by Chiesa et al. [24] and Gulen [36].

The 3PRH cycle layout used for CCGT validation in WTEMP is shown in Fig. 4. Outlet of HP steam turbine (S1) was mixed with the superheated IP steam and the resulting flow was

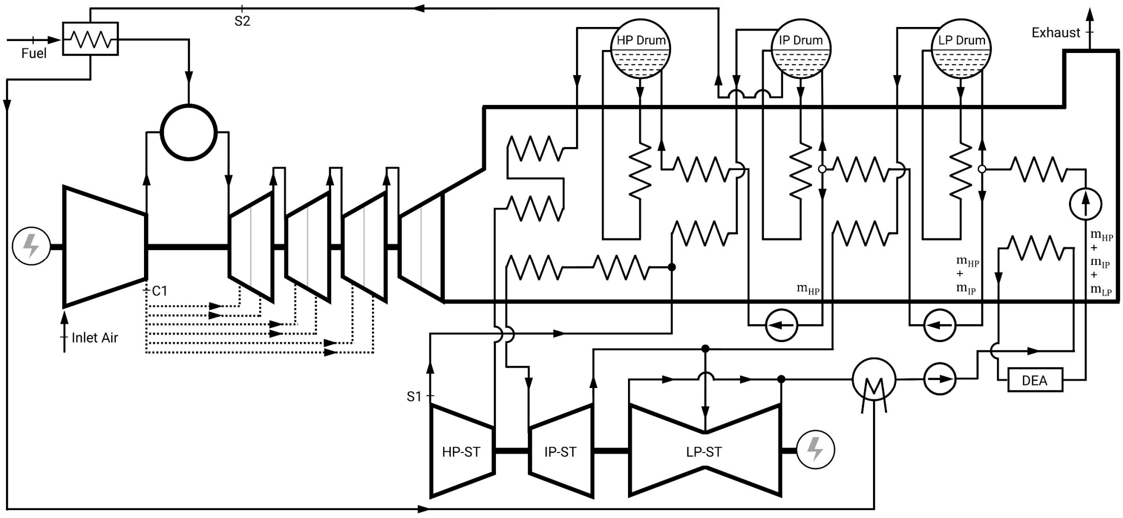

FIGURE 4: DETAILED SCHEMATIC DIAGRAM OF THE PRACTICAL 3PRH CCGT IN WTEMP FOR VALIDATION

TABLE 2: PARAMETERS IN GT CYCLE MODEL

Parameter	Value
Inlet Air Temperature (°C)	15
Inlet Air Pressure (bar)	1.013
Relative Humidity (%)	60
Compressor polytropic efficiency (%)	90
Turbine polytropic efficiency (%)	90
Combustion efficiency (%)	99.9
Combustor pressure drop (%)	5
Mechanical Efficiency (%)	99.5
Blade metal temperature (°C)	890
Generator Efficiency (%)	98.85

TABLE 3: PARAMETERS IN BOTTOMING CYCLE MODEL

Parameter	Value
LP Pressure (bar)	5
IP Pressure (bar)	45
HP Pressure (bar)	160
Economizer sub-cool (°C)	8
Evaporator pinch-point ΔT(°C)	10
Superheater approach ΔT(°C)	15
HP Steam Turbine Efficiency (%)	90
IP Steam Turbine Efficiency (%)	91
LP Steam Turbine Efficiency (%)	91
Water Side Pressure Drop (%)	1.5
Heat loss SH, EV & EC (%)	0.25
Pump Adiabatic Efficiency (%)	85
Electrical Engine Efficiency (%)	97

admitted in the IP steam turbine after passing through two reheat heat exchangers. Fuel was preheated in an external heat exchanger using water (S2) from the IP steam drum, as shown in Fig. 4. Compressor bleed air (C1 in Fig. 4) for turbine cooling was extracted from the final row at discharge temperature. Six out of eight turbine rows (first three stages) were cooled in this work [23,24]. The last two rows did not require cooling owing to temperature drop from expansion.

TIT was defined as the temperature at the combustor outlet or first stator inlet. TIT was then calibrated through heat balance in WTEMP to reach desired TOT with minimum error in efficiency and power. As a result of continuous past efforts to increase TIT, most modern H-Class CCGTs have TIT of 1600°C or higher. Mitsubishi has already commercialized CCGT with 1650°C TIT. in 2020 [37] and has a development program towards 1700°C TIT [38]. Similarly, the HA class of plants from GE are advertised with 1600°C TIT technology. Apart from TIT, TOT is another important parameter in CCGTs. Practical HRSGs are typically fed with TOT in the range of 550-650°C [36], and the latest industrial CCGTs can even have TOT higher than 650°C [35]. Therefore, a maximum live steam temperature of 640°C was used for M701JAC and 9HA.02 and 620°C were used for GT36-S5 in the validation. Also, a condenser pressure of 0.04 bar was assumed for M701JAC and 9HA.02 and 0.06 bar was assumed for GT36-S5. Due to the unavailability of these data in the current year from OEM, reasonable values had to be taken based on literature and OEM data from previous years. The final results of the validation process are shown in Table 4. All the error values between OEM and WTEMP data were less than 3%.

2.4. Cooling Solutions and Layouts

Ansaldo GT36-S5 was selected as the reference CCGT to study performance improvement with steam cooling and PGC in practical CCGTs. For CCGT with a PGC combustor, the conventional isobaric combustor was replaced with the PGC model described in section 2.1, and then six different cooling solutions (apart from conventional OLAC) were investigated for conventional and PGC-based CCGT. These cooling strategies are described below.

1. Open-loop air cooling (OLAC): Both the stator and rotor are cooled by compressor bleed air, and cooling air is mixed with the main gas flow in the turbine.
2. Open-loop steam cooling (OLSC): Both stator and rotor are cooled by steam, followed by the mixing of steam with the main gas flow in the turbine.
3. Closed loop steam cooling (CLSC): Both stator and rotor are steam cooled, but steam is readmitted in the steam cycle after cooling the blade without mixing in turbine flow.

TABLE 4: RESULTS OF CCGT MODEL VALIDATION IN WTEMP.

	GT36-S5 (Ansaldo Energia)		**M701JAC** (Mitsubishi)		**9HA.02** (General Electric)	
Parameter	**OEM** [35]	**WTEMP**	**OEM** [35]	**WTEMP**	**OEM** [15]	**WTEMP**
Simple cycle power (MW)	538.0	541.1 (0.58)	574.0	570.9 (-0.55)	571.0	571.4 (0.06)
Simple cycle efficiency (%)	42.8	43.79 (2.32)	43.4	43.42 (0.04)	44.0	43.1 (-2.07)
Pressure ratio	26.0	26.0	25.0	25.0	23.8	23.8
TOT (°C)	621.0	612.1 (-1.43)	646.0	647.9 (0.29)	640.0	647.4 (1.16)
TIT (°C)	-	1570	-	1640	-	1610
Exhaust mass flow (kg/s)	1020	1020	1024	1024	1040	1040
Combined cycle power (MW)	760.0	762.1 (0.28)	840.0	825.1 (-1.77)	838.0	828.9 (-1.09)
Combined cycle efficiency (%)	62.6	62.6 (0)	64.0	63.7 (-0.46)	64.1	63.5 (-0.95)
Gas Turbine Power (MW)	533.0	528.3 (-0.88)	570.9	556.8 (-2.47)	561.0	556.9 (-0.73)
Steam Turbine Power (MW)	227.0	233.8 (3.0)	269.1	268.3 (-0.30)	277.0	272.0 (-1.82)
Non-chargeable cooling flow (%)	-	8.6	-	10.2	-	9.3
Chargeable cooling flow (%)	-	5.9	-	6.3	-	5.9

- Numbers inside the bracket show the error in percentage.
- Non-chargeable cooling flow is the cooling flow for the first stator and all other cooling flows are chargeable. Values are given as a percentage of compressor inlet air.

4. Mixed-loop steam cooling (MLSC): Stator is steam-cooled, and rotor is air-cooled. Stator cooling steam is readmitted in the steam cycle after cooling.
5. MLSC+CBAC1: MLSC with compressor bleed air cooling (CBAC) through a parallel HP evaporator.
6. OLAC+CBAC1: OLAC with compressor bleed air cooling (CBAC) through a parallel HP evaporator.
7. OLAC+CBAC2: OLAC with compressor bleed air cooling (CBAC) through a parallel IP economizer.

These cooling strategies are described in Table 5. Representative schematics of the PGC combined cycle layouts are shown in Figures 5, 6 and 7 for three different cooling solutions. The compressor discharge temperature in this work was 513°C for all cases, as the pressure ratio was constant. Note that for CBAC1, the compressor bleed (C1) air was cooled in a parallel HP evaporator by HP water extracted upstream of the HP drum (S3 in Fig. 5). In this case, the cooling air temperature was reduced to 356°C, as determined by the saturation temperature and the pinch point. In the case of CBAC2, the cooling air was cooled down through IP water using a parallel IP economizer and in this case, the outlet temperature of cooling air was set as 150°C.

For turbine blade cooling with steam, steam (S4 in Fig. 6 & 7) was extracted from the outlet of the HP steam turbine [22,24]. After cooling the turbine blades, this steam was mixed with the outflow of the first reheat heat exchanger. The pressure drop of cooling steam was accounted for during this mixing process.

TABLE 5: DIFFERENT COOLING INTEGRATION STRATEGIES.

Cooling Solution	Stator Cooling Medium	Rotor Cooling Medium
OLAC	Air(513°C)	Air (513°C)
OLSC	Steam	Steam
CLSC	Steam	Steam
MLSC	Steam	Air (513°C)
MLSC+CBAC1	Steam	Air (356°C)
OLAC+CBAC1	Air (356°C)	Air (356°C)
OLAC+CBAC2	Air (150°C)	Air (150°C)

For OLSC, where steam was mixed with the main turbine flow, the intermediate level pressure of 45 bar was sufficient enough to allow the steam entry into the turbine, especially with pressure gain.

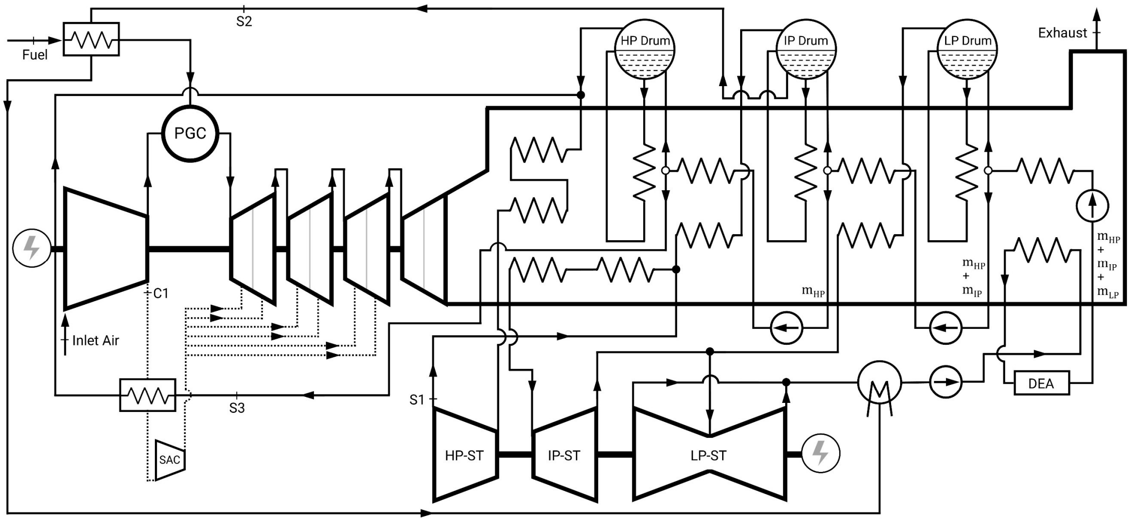

FIGURE 5: SCHEMATIC DIAGRAM OF THE VALIDATED CCGT WITH OLAC+CBAC1.

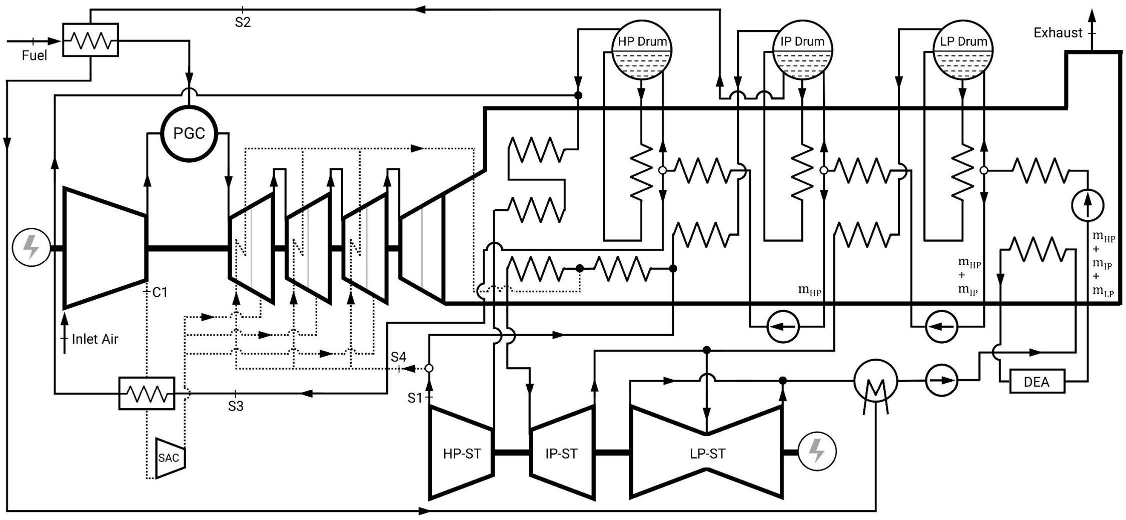

FIGURE 6: SCHEMATIC DIAGRAM OF THE VALIDATED CCGT WITH MLSC+CBAC1.

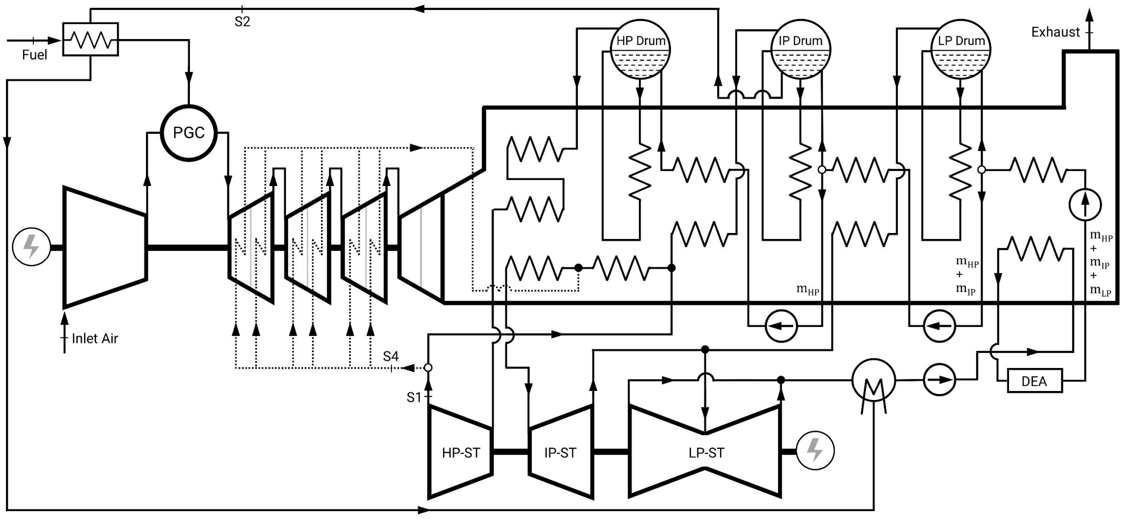

FIGURE 7: SCHEMATIC DIAGRAM OF THE VALIDATED CCGT WITH CLSC

Methane was used as fuel in all simulations. Simulations were performed with conventional CCGT with an isobaric combustor and CCGT with a pressure gain combustor with six different values of pressure gain determined by the combustor injection pressure loss. Injection pressure loss is a major issue in PGC combustors and can completely nullify the ideal advantage of PGC combustion [7]. Injection pressure loss was varied from 0-50% in steps of 10. Thereafter, seven cooling strategies mentioned in Table 5 were simulated for each case of PGC combustor and conventional isobaric combustor. Note that all PGC layouts with cooling air from the compressor (C1) required the secondary air compressor (SAC) to compensate for the pressure gain, while the CLSC configuration (Fig. 7) had no SAC. In the case of SAC compression, the cooling air temperature at the inlet of the initial blade rows was slightly higher than the compressor discharge temperature of 513°C.

3. RESULTS AND DISCUSSION

This section describes the impact of seven different cooling solutions on conventional CCGT and CCGT with PGC combustor at six different pressure gain values.

3.1. Independent Impact of Steam Cooling and PGC on CCGT Performance

The independent impact of the two technologies, steam cooling integration and PGC combustion, on the performance of CCGT is shown in Fig. 8(a) and (b), respectively. Firstly, looking at the impact of steam cooling (with conventional combustor) in Fig. 8(a), it can be seen that the proposed solutions can significantly increase the efficiency and specific work of CCGT. The biggest impact on CCGT performance comes from CLSC, which increases efficiency to 64.2% (1.6 p.p. increment) and specific work by over 152 kJ/kg$_{air}$. Next to CLSC, MLSC+CBAC1 has the largest positive impact on CCGT performance. It increases cycle efficiency to 63.6% (1 p.p. increment) and specific work by 100 kJ/kg$_{air}$. Other solutions have an intermediate effect on efficiency and specific work, with OLSC being an exception. OLSC increases the specific work by 118 kJ/kg$_{air}$ but reduces the efficiency by 0.8 p.p. due to the mixing losses. MLSC, which includes rotor cooling by compressor bleed air and stator cooling with steam in a closed loop, shows performance benefits midway between conventional

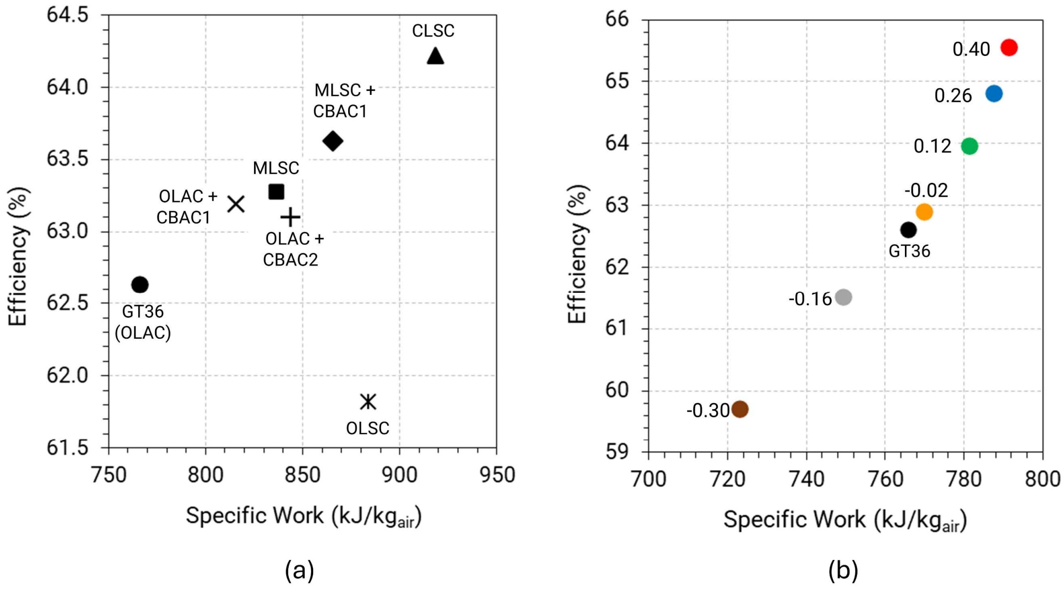

FIGURE 8: PERFORMANCE IMPROVEMENT IN CCGT WITH DIFFERENT STEAM INTEGRATION SOLUTIONS (a) AND WITH PGC COMBUSTION (NUMBERS NEXT TO SYMBOL ARE P_{gain} VALUES) (b)

OLAC and CLSC. When MLSC is augmented by cooling the compressor bleed air using a parallel HP evaporator in MLSC+CBAC1, it facilitates further improvements in both efficiency and specific work, which shows the significance of cooling the compressor bleed air. With a lower temperature of cooling air, less cooling flow is required for the same heat transfer, which reduces the cooling-associated penalty on the GT performance. Finally, comparing the OLAC+CBAC1 and OLAC+CBAC2, both show performance improvement over conventional OLAC, but efficiency improvement is higher in the former, while the specific work improvement is higher in the latter. This difference is due to the fact that in OLAC+CBAC2, entry temperature of cooling flow in the turbine is less, leading to lesser cooling mass flow and thus increased TOT (Fig. 11(a)), because of which the GT power is increased (Fig. 11(b)). However, as the maximum live steam temperature is limited to 620°C, some thermal energy is not recovered by the bottoming cycle, leading to lower efficiency. However, in both OLAC+CBAC1 and OLAC+CBAC2, the advantage of reducing cooling air temperature is quite evident.

Replacing a conventional combustor with a PGC combustor while using the conventional OLAC for turbine cooling also enhances the CCGT performance significantly, as shown in Fig. 8(b). The compressor pressure ratio was maintained constant in this work, and therefore, the combustor injection pressure loss (in %) of 0,10,20,30,40 and 50 resulted in the P_{gain} of 0.40, 0.26, 0.12, -0.02, -0.16 and -0.30. An injection pressure loss of 30% results in a net pressure drop across the combustor because the P_{gain} in the combustor is insufficient to compensate for the injection pressure loss. At the highest P_{gain} of 0.40, the cycle efficiency increases to 65.6%, a 2.9 p.p. increase, which is higher than the maximum increment of 1.6 p.p. obtained with CLSC with a conventional combustor. Also, P_{gain} of 0.40 increases specific work by 26.6 kJ/kg$_{air}$, which is lower than the specific work benefit produced by only CLSC. With a decrease in P_{gain}, both efficiency and specific work continue to decrease, eventually dropping down below GT36. It can be inferred from Fig. 8 that when implemented as independent solutions, steam cooling is better for increasing specific work, and PGC is better for increasing efficiency.

3.2. Combined Impact of Steam Cooling and PGC on CCGT Performance

Figure 9 shows the results of the CCGT performance by implementing various steam cooling solutions and PGC combustors with different pressure gains. All the data points with the same pressure gain are coloured the same, and the grey line connects all data points with the same cooling strategy. Data points of GT36 with conventional combustor and different cooling strategies (shown in Fig. 8(a)) are shown in black color with the same symbol. It is clearly evident from Fig. 9 that implementing steam cooling and PGC together enables remarkably high improvements in both efficiency and specific work due to the synergistic effect. For instance, implementing CLSC together with PGC with a P_{gain} of 0.40 increases the efficiency to 67.2% (4.54 p.p. improvement over GT36) and specific work by 194.5 kJ/kg$_{air}$. For comparison, the highest efficiencies reported by OEMs of CCGT powerplants are 64% for M701JAC by Mitsubishi [35] and 64.1% for 9HA.02 by General Electric [15]. This 4.54 p.p. efficiency rise is more than the highest gain of 2.9 p.p. achieved independently by PGC. Similarly, the rise in specific work by 194.5 kJ/kg$_{air}$ is higher than the increment of 152 kJ/kg$_{air}$ achieved by steam cooling alone. It clearly shows that both technologies complement each other, resulting in very high-performance improvement in CCGT. Even with P_{gain}=0.26 at 10% pressure loss in the PGC combustor, CCGT efficiency with CLSC is higher than GT36 by 3.8 p.p., and specific work is higher by 184 kJ/kg$_{air}$. After CLSC, MLSC+CBAC1 is the most promising cooling technology in terms of theoretical benefits. Although CLSC gives the highest theoretical benefit, its implementation in practical gas turbines is

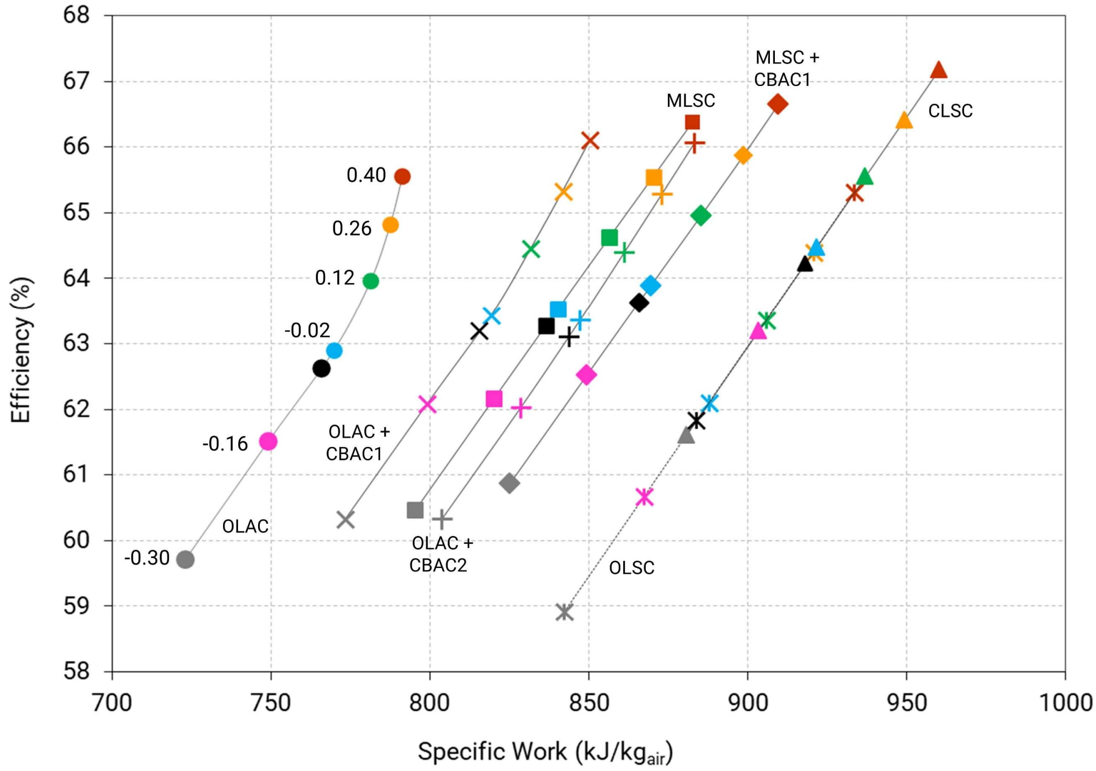

FIGURE 9: PERFORMANCE IMPROVEMENT IN GT36 WITH IMPLEMENTATION OF BOTH STEAM COOLING AND PGC COMBUSTORS AT DIFFERENT PRESSURE GAINS. EACH COLOR REPRESENT A SPECIFIC PRESSURE GAIN VALUE. EACH LINE CONNECTS DATA POINTS WITH SAME COOING STRATEGY. OLSC LINE IS DOTTED BECAUSE OF PARTIAL OVERLAP WITH CLSC

very challenging, in particular for rotors, because it is difficult to extract steam from high-speed rotor blades. Comparatively, closed-loop steam cooling of only stator blades is a more practical solution. MLSC+CBAC1 uses this approach and additionally cools the compressor bleed air through the HP evaporator. In the most optimistic case of P_{gain}=0.40, MLSC+CBAC1 enhances efficiency by 4 p.p. and specific work by 117 kJ/kg$_{air}$. Realistically, a 10% pressure loss in a PGC device could be considered a practically achievable value in the near future with the ongoing research advancements in PGC technology. This 10% pressure loss in PGC corresponds to P_{gain}=0.26, which, when integrated with MLSC+CBAC1, is capable of delivering an efficiency gain of 3.2 p.p. and a specific work gain of 132.8 kJ/kg$_{air}$. Cooling the compressor bleed air in CBAC1 mode is also more practical than CLSC for the rotor. Moreover, the outlet temperature of cooling air in the parallel HP evaporator is automatically controlled based on saturation pressure and the evaporator pinch point. However, in MLSC+CBAC1, rotor air is still cooled by the steam from the bottoming cycle, so it can introduce some practical challenges because of the coupling between rotor air and the bottoming cycle. On the other hand, MLSC, in which the blade cooling air can be simply channelled through the rotor, could be considered a more practical solution than other ones. With 10% combustor injection pressure loss and P_{gain}=0.26, MLSC can increase the efficiency of GT36 by 2.9 p.p. and specific work by 104.6 kJ/kg$_{air}$. OLAC+CBAC2 also provides comparable enhancement, however, CBAC2 could pose practical challenges in rotor cooling media management because of the fixed outlet temperature of the cooling air.

Finally, Fig. 9 also shows that the curve connecting all the points of the same steam cooling strategy becomes more linear towards the right. This shows a proportional increase in efficiency and specific work with an increase in pressure gain. It implies that in the simple OLAC approach, the specific work can suffer from the negative impact of the increased cooling flow with pressure gain. This effect can be mitigated by employing more complex cooling schemes like the ones presented in this paper. In particular the use of steam as cooling media can restore the linear increment of efficiency and specific work with pressure gain.

3.3. Impact of Steam Cooling and PGC on Cycle Parameters

This section describes the variation of key cycle parameters with different steam cooling solutions. Figure 10 shows the cooling flow for each turbine row for different strategies for three combustors: GT36 with conventional combustor (a), GT36 with a PGC combustor with no injection pressure loss (for maximum P_{gain}) (b) and GT36 with a PGC combustor having 20% injection pressure loss (for a realistic P_{gain}) (c). Note that OLSC has not been discussed here due to its poor efficiency (Fig. 8(a)). The highest amount of cooling flow is required with OLAC in all three configurations because more cooling air is required when it enters the turbine at compressor discharge temperature (513°C). In MLSC, stator rows have nearly half the cooling flow, as compared to those in OLAC, because of the high specific heat of steam (Fig. 3). For the same reason, all cooling flows have been reduced significantly in CLSC, when all the rows are steam cooled. The effect of compressor bleed air cooling can also be seen in going from MLSC to MLSC+CBAC1. All rotor cooling flows in the latter are reduced due to lower cooling flow temperature (356°C), while that of the stator (steam cooled) remains the same. Similarly, in all configurations, OLAC+CBAC1 has a higher cooling flow compared to OLAC+CBAC2 due to a higher cooling flow temperature of 356°C instead of 150°C. Moreover, the effect of pressure gain can also be seen in Fig. 10(a) & (b), more easily in OLAC, where the first stator requires higher cooling flow due to increased cooling flow temperature from secondary compression (as shown in Fig. 5 & 6). The effect of a higher PGC expansion ratio can be seen as well in the third stage where the cooling flow is nearly zero in PGC without loss (Fig. 10(b)). This is because of the high expansion ratio, where initial stages expand the working fluid to a temperature low enough so that the subsequent stage does not require cooling. When 20% combustor injection pressure loss is introduced in Fig. 10(c), the expansion ratio decreases again, making the cooling of the third stage also necessary.

Figures 11(a), (b) & (c) show the TOT, GT power and ST power, respectively, for conventional CCGT, CCGT with PGC with no injection pressure loss and CCGT with PGC with 20% injection pressure loss. In Fig. 11(a), as would be expected, OLAC has the lowest TOT because of the highest dilution from the cooling flow. With subsequent cooling strategies, the cooling flow reduces and due to less dilution, the TOT of the gas turbine cycle increases. Maximum TOT occurs in CLSC for all three configurations because there is no mixing with the main flow. A

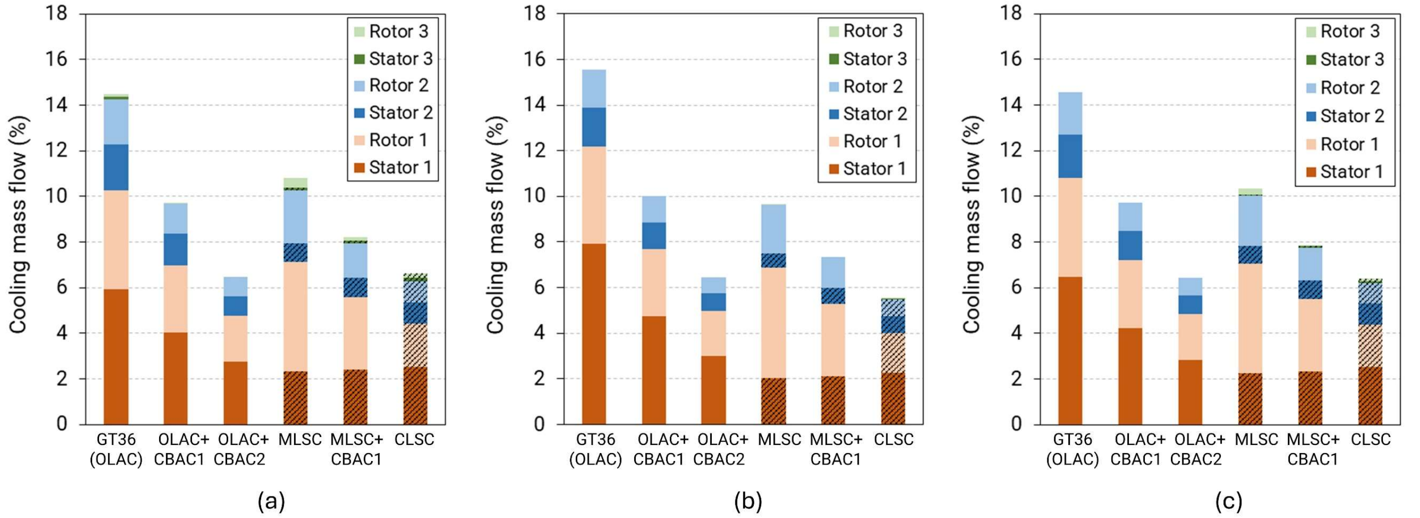

FIGURE 10: COOLING FLOW RATES FOR ALL COOLED TURBINE ROWS: CONVENTIONAL CCGT (a), CCGT WITH PGC COMBUSTOR WITHOUT INJECTION PRESSURE LOSS (b) AND CCGT WITH PGC COMBUSTOR WITH 20% INJECTION PRESSURE LOSS (c). STRIPPED COLUMNS ARE STEAM-COOLED ROWS, AND UNSTRIPPED COLUMNS ARE AIR-COOLED ROWS.

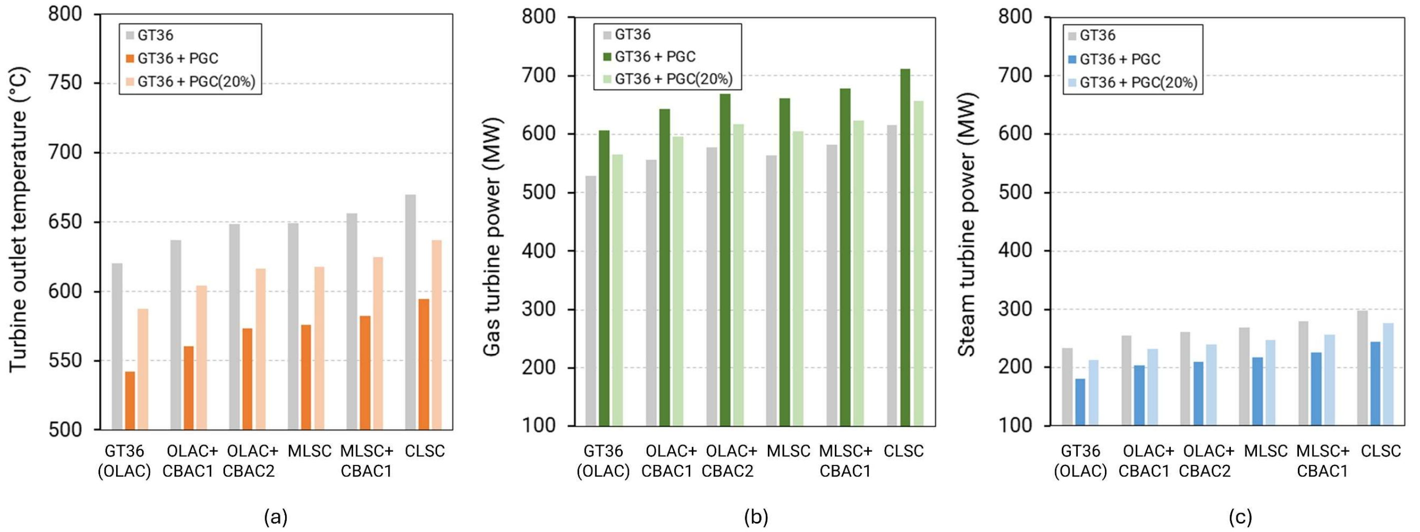

FIGURE 11: GAS TURBINE OUTLET TEMPERATURE (a), GAS TURBINE POWER (b) AND STEAM TURBINE POWER (b) FOR THREE DIFFERENT CASES. PGC(20%) IS THE PGC COMBUSTOR WITH 20% INJECTION PRESSURE LOSS.

higher TOT increases the steam cycle work, which can be seen in Fig. 11(c), which shows a similar trend as TOT. Looking at the individual configuration, PGC without loss has the lowest TOT due to a high expansion ratio resulting from high-pressure gain (P_{gain}=0.40) [7,12]. However, with a 20% loss, the pressure gain is reduced ((P_{gain}=0.12), leading to higher TOT. The biggest impact of reduced cooling flow with different steam cooling integration strategies is reflected in the form of increased gas turbine work, as shown in Fig. 11 (b). For each configuration, as the cooling flow is reduced, the gas turbine work increases. Therefore, OLAC, with the highest cooling flow, shows minimum gas turbine work among each of the three configurations. On the other hand, CLSC with minimum cooling flow allows the gas turbine to produce highest work, which is also reflected in the efficiency. This is due to the reduction in cooling associated penalty on the gas turbine performance.

The total heat transferred from the gas turbine cycle to the steam cycle through blade cooling is shown in Fig. 12 for the same three configurations shown in Fig. 10 and 11. Note that Fig. 12 does not include the heat exchanged with the bottoming cycle through fuel preheating, as it is already included in the base case GT36 and all other configurations. For the sake of perspective, the value of heat exchanged through fuel preheating in this work was in the range of 13-16 MJ for different test cases. The slight difference in this heat is due to the different fuel flow in the combustor with changing combustor inlet airflow for the fixed TIT. CLSC, in which all blade rows are steam cooled in a closed loop, the total heat transferred is maximum. CLSC is followed by MLSC+CBAC1, in which all stator heat, along with some heat from compressor bleed air, is transferred to the steam cycle. Next, MLSC and OLAC+CBAC2 transfer comparable amounts of heat, while OLAC+CBAC1 has minimum heat transfer from the topping cycle to the bottoming cycle because of the high temperature of cooling air outlet temperature of 356°C, as set by steam saturation pressure. On comparing Fig. 9 and Fig. 12, it can be seen the steam integration strategy that transfers more heat from the gas turbine to the bottoming steam cycle is likely to produce higher efficiency for the entire cycle. Turbine cooling through conventional compressor-bleed air prevents a part of useful working fluid from contributing to cycle work generation (also referred to as chargeable cooling flow), thus reducing cycle efficiency. Cooling integration with steam allows more working fluid to produce more work in the gas turbine while also increasing the steam cycle work through the heat recovered from the blades, thereby increasing the overall combined cycle efficiency.

4. CONCLUSION

This study investigated the impact of different strategies of integrating turbine blade cooling in combined cycle gas turbines (CCGT) with pressure gain combustion (PGC) to understand the potential performance improvements. Cooling strategies were implemented in a validated H-class CCGT model at different values of PGC pressure gain. The following conclusions can be drawn from this work.

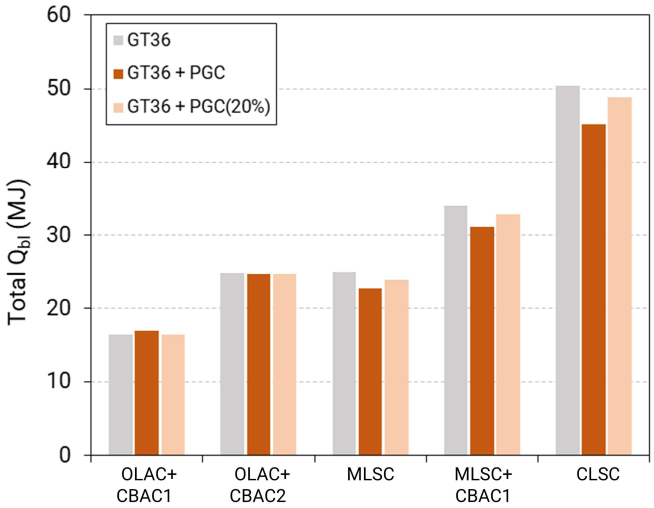

FIGURE 12: TOTAL HEAT TRANSFER FROM GAS TURBINE CYCLE TO STEAM CYCLE THROUGH BLADE COOLING FOR THREE CASES.

1. If PGC and steam cooling are to be implemented independently in CCGT powerplants, PGC is better in increasing efficiency, while steam cooling offers better specific work enhancement.
2. Closed loop steam cooling (CLSC), in which both stator and rotor are steam cooled and steam is readmitted in the bottoming cycle offers the highest performance gain in CCGT with conventional combustor. It can increase cycle efficiency by 1.6 p.p. and specific work by 152 kJ/kg_{air}. Next to CLSC, MLSC+CBAC1, in which the stator is steam-cooled and compressor bleed air for rotor cooling is cooled through a parallel HP evaporator, offers the highest performance improvement in conventional CCGTs.
3. The adoption of Compressor Bleed Air Cooling to decrease the coolant temperature has a direct impact on the efficiency and specific work: starting from a Compressor Discharge Temperature of 513°C, reducing the cooling temperature to 356°C (CBAC1) has the main impact on efficiency (+0.56 p.p.), while a stronger heat exchange to bottoming cycle, reaching down to 150°C (CBAC2) has a major impact in reducing the cooling flow requirements, with a more relevant impact on the specific work (+77.9 kJ/kg_{air}).
4. Implementing both PGC technology and steam cooling together in a CCGT can significantly enhance the efficiency and work output due to the synergistic effect of both technologies. At an optimistic pressure gain of 0.40, the efficiency of an H-class CCGT can be increased from 62.6% to 67.2% (4.54 p.p. increment), and specific work can be increased by 194.5 kJ/kg_{air} by using CLSC.
5. Mixed loop steam cooling (MLSC) can be considered the most practical strategy in CCGT with PGC combustor. At a realistically achievable pressure gain of 0.26, it can increase the efficiency of CCGT by 2.9 p.p. and specific work by 104.6 kJ/kg_{air}.
6. CLSC is able to transfer the highest amount of heat from blade cooling into the steam turbine cycle in CCGT with both conventional and PGC combustors.

7. Employing PGC combustion technology and integrating blade cooling with the steam bottoming cycle, together can provide a pathway to achieve higher than 65% CCGT efficiency.

5. ACKNOWLEDGEMENT

This project has received funding from the European Union's Horizon 2020 research and innovation programme under the Marie Skłodowska-Curie grant agreement No: INSPIRE-956803. The financial support received from the European Union is gratefully acknowledged.

6. REFERENCES

[1] Gulen, S. C., 2018, "Beyond Brayton Cycle: It Is Time to Change the Paradigm," J. Eng. Gas Turbines Power, **140**(11), pp. 1–10.

[2] Neumann, N., and Peitsch, D., 2019, "Potentials for Pressure Gain Combustion in Advanced Gas Turbine Cycles," Appl. Sci., **9**(16).

[3] Akbari, P., and Nalim, M. R., 2009, "Review of Recent Developments in Wave Rotor Combustion Technology," J. Propuls. Power, **25**(4), pp. 833–844.

[4] Lu, F. K., Braun, E. M., and Powers, J., 2014, "Rotating Detonation Wave Propulsion: Experimental Challenges, Modeling, and Engine Concepts," J. Propuls. Power, **30**(5), pp. 1125–1142.

[5] Musielak, D., 2015, "Pulse Detonation Engine and Continuous Detonation Wave Engines," pp. 1–4.

[6] Gutmark, E. J., 2021, "Pressure Gain Combustion," Shock Waves, **31**(7), pp. 619–621.

[7] Dubey, A., Sorce, A., and Stathopoulos, P., 2024, "A Comprehensive Thermodynamic Analysis of Gas Turbine Combined Cycles With Pressure Gain Combustion Based on Humphrey Cycle," J. Eng. Gas Turbines Power, **147**(February), pp. 1–39.

[8] Neumann, N., Woelki, D., and Peitsch, D., 2019, "A Comparison of Steady-State Models for Pressure Gain Combustion in Gas Turbine Performance Simulation," *Proceedings of Global Power and Propulsion Society*, Beijing.

[9] Nordeen, C. A., Schwer, D., Schauer, F., Hoke, J., Barber, T., and Cetegen, B., 2014, "Thermodynamic Model of a Rotating Detonation Engine," Combust. Explos. Shock Waves, **50**(5), pp. 568–577.

[10] Stathopoulos, P., 2020, "An Alternative Architecture of the Humphrey Cycle and the Effect of Fuel Type on Its Efficiency," Energy Sci. Eng., **8**(10), pp. 3702–3716.

[11] Heiser, W. H., and Pratt, D. T., 2002, "Thermodynamic Cycle Analysis of Pulse Detonation Engines," J. Propuls. Power, **18**(1), pp. 68–76.

[12] Stathopoulos, P., 2018, "Comprehensive Thermodynamic Analysis of the Humphrey Cycle for Gas Turbines with Pressure Gain Combustion," Energies, **11**(12).

[13] Nalim, M. R., 2002, "Thermodynamic Limits of Work and Pressure Gain in Combustion and Evaporation Processes," J. Propuls. Power, **18**(6), pp. 1176–1182.

[14] Ol'khovskii, G. G., 2021, "The Most Powerful Power-Generating GTUs (a Review)," Therm. Eng. , **68**(6), pp. 490–495.

[15] 2024, "General Electric 9HA.02 Gas Turbine" [Online]. Available:https://www.gevernova.com/gaspower/products/gas-turbines/9ha. [Accessed: 30-Nov-2024].

[16] Gulen, S. C., 2017, "Pressure Gain Combustion Advantage in Land-Based Electric Power Generation," J. Glob. Power Propuls. Soc., **1**.

[17] Holley, A., 2017, "Combined Cycle Power Generation Employing Pressure Gain Combustion."

[18] Giuffrida, A., Chiesa, P., and Sordillo, A. P., 2024, "A Thermodynamic Study of Pressure Gain Combustion in Combined Cycles," *79th Annual ATI Congress*, Genova, Italy.

[19] Dubey, A., Purushothaman, S., Sorce, A., and Traverso, A., 2022, "A Review of Recent Advances in the Combustor and Blade Cooling Methods for Pressure Gain Applications," *Joint Meeting of International Workshop on Detonation for Propulsion (IWDP) and International Constant Volume and Detonation Combustion Workshop (ICVDCW)*, Berlin, Germany.

[20] Dubey, A., and Sorce, A., 2024, "Exergy Analysis of Gas Turbine Open Cycle with Pressure Gain Combustion Based on Humphrey Cycle," *ATI Congress 2024*, Genova, Italy.

[21] Jordal, K., Torbidoni, L., and Massardo, A. F., 2001, "Convective Blade Cooling Modelling for the Analysis of Innovative Gas Turbine Cycles," *Volume 2: Coal, Biomass and Alternative Fuels; Combustion and Fuels; Oil and Gas Applications; Cycle Innovations*, American Society of Mechanical Engineers, New Orleans, Louisiana, USA.

[22] Watson, D. T., and Ritchey, I., 1997, "Thermodynamic Analysis of Closed Loop Cooled Cycles," *Proceedings of the ASME Turbo Expo*, Orlando, Florida, USA.

[23] Ghigliazza, F., Traverso, A., and Massardo, A. F., 2009, "Thermoeconomic Impact on Combined Cycle Performance of Advanced Blade Cooling Systems," Appl. Energy, **86**(10), pp. 2130–2140.

[24] Chiesa, P., and Macchi, E., 2004, "A Thermodynamic Analysis of Different Options to Break 60% Electric Efficiency in Combined Cycle Power Plants," J. Eng. Gas Turbines Power, **126**(4), pp. 770–785.

[25] Kotowicz, J., Job, M., and Brzeczek, M., 2015, "The Characteristics of Ultramodern Combined Cycle Power Plants," Energy, **92**, pp. 197–211.

[26] Sanjay, Singh, O., and Prasad, B. N., 2008, "Influence of Different Means of Turbine Blade Cooling on the Thermodynamic Performance of Combined Cycle," Appl. Therm. Eng., **28**(17–18), pp. 2315–2326.

[27] Kotowicz, J., Brzęczek, M., and Job, M., 2018, "The Thermodynamic and Economic Characteristics of the Modern Combined Cycle Power Plant with Gas Turbine Steam Cooling," Energy, **164**, pp. 359–376.

[28] Tsutsumi AT, MA, M., AT, Y., Nakamoto YU, Y., and MA, U., 2003, "Description of the Latest Combined Cycle Power Plant with G Type Gas Turbine Technology in the Philippines," Mitsubishi Heavy Ind. Tech., **40**(4), pp. 1–5.

[29] Smith, R. W., Polukort, P., Maslak, C. E., Jones, C. M.,

and Gardiner, B. D., 2001, *Advanced Technology Combined Cycles*, Schenectady, NY.

[30] Horlock, J. H., Watson, D. T., and Jones, T. V., 2001, "Limitations of Gas Turbine Performance Imposed by Large Turbine Cooling Flows," J. Eng. Gas Turbines Power, **123**(3), pp. 487–494.

[31] Kurzke, J., 2002, "Performance Modeling Methodology: Efficiency Definitions for Cooled Single and Multistage Turbines," Am. Soc. Mech. Eng. Int. Gas Turbine Institute, Turbo Expo IGTI, **1**, pp. 85–92.

[32] Wilcock, R. C., Young, J. B., and Horlock, J. H., 2005, "The Effect of Turbine Blade Cooling on the Cycle Efficiency of Gas Turbine Power Cycles," J. Eng. Gas Turbines Power, **127**(1), pp. 109–120.

[33] Traverso, A., Massardo, A. F., Cazzola, W., and Lagorio, G., 2004, "Widget-Temp: A Novel Web-Based Approach For Thermoeconomic Analysis And Optimization Of Conventional And Innovative Cycles," *Proceedings of ASME Turbo Expo 2004*, Vienna, Austria.

[34] Ghigliazza, F., Traverso, A., and Massardo, A. F., 2009, "Thermoeconomic Impact on Combined Cycle Performance of Advanced Blade Cooling Systems," Appl. Energy, **86**(10), pp. 2130–2140.

[35] 2024, "Turbomachinery International: Handbook 2024," **64**(6).

[36] Gulen, S., 2019, *Gas Turbine Combined Cycle Power Plants*, CRC Press, Boca Raton.

[37] Morimoto, K., Matsumura, Y., Suzuki, K., Wakazono, S., Katoka, M., and Yuri, M., 2021, "Operation Status of 1650 ° C Class M501JAC Gas Turbine at T-Point 2 Power Plant Demonstration Facility," Mitsubishi Heavy Ind. Tech. Rev., **58**(3), pp. 1–10.

[38] Ito, E., Okada, I., Tsukagoshi, K., Muyama, A., and Masada, J., 2010, "Development of Key Technologies for the Next Generation Gas Turbine," *ASME Turbo Expo 2010: Power for Land, Sea, and Air*, Glasgow, UK, pp. 847–860.